Supporting Information for

Quantitative analysis of weak antilocalization effect of topological surface states in topological insulator $BiSbTeSe_2$

Hui Li[1], Huan-Wen Wang[1], Yang Li[1], Huachen Zhang[1], Shuai Zhang[2,3], Xing-Chen Pan[2,3], Bin Jia[2,3], Fengqi Song[2,3], Jiannong Wang[1,4]*

[1]*Department of Physics, the Hong Kong University of Science and Technology, Clear Water Bay, Hong Kong, China*

[2]*National Laboratory of Solid State Microstructures, School of Physics, Nanjing University, Nanjing, 210093, China*

[3]*Collaborative Innovation Center of Advanced Microstructures, Nanjing University, Nanjing, 210093, China*

[4]*William Mong Institute of Nano Science and Technology, the Hong Kong University of Science and Technology, Clear Water Bay, Kowloon, Hong Kong, China*

* Correspondence and requests for materials should be addressed to J. W. (email: phjwang@ust.hk, Tel: (852) 2358 7497, Fax: (852) 2358 1652).

1. Zeeman effect on the split of topological surface states

Previous studies have proved that the *g*-factor of the topological surface state of topological insulators is strongly materials dependent. For example, the *g*-factor of the topological surface state is about 18 for Bi_2Se_3, while is about -6 for Sb_2Te_2Se[1]. Even no exact value of *g*-factor of the topological surface state of $BiSbTeSe_2$ system was reported, there are still some experimental findings suggesting the *g*-factor of the topological surface state of $BiSbTeSe_2$ system should be very small, such as no evident shift of the zeroth Landau level (LL) was observed under B = 30 T in $BiSbTeSe_2$ flakes[2], small Zeeman gap with the value of about 1 meV in $BiSbTeSe_2$[3].

On the other hand, for ideal helical Dirac fermions, the Zeeman shift of the *n*-th LL, $\Delta E_{n\neq 0} \cong \pm \frac{(g_s \mu_B B/2)^2}{\sqrt{2|e|\hbar v^2 nB}}$, is smaller than that of the zeroth LL of $E_{n=0} = -g_s \mu_B B/2$ and decreases dramatically with increasing *n*, where g_s is the Lande *g*-factor, μ_B is the Bohr magneton, B is the magnetic field, v is the electron velocity[1]. For our $BiSbTeSe_2$ system, as shown in the ARPES results in Figure S2 below, the energy difference between the Fermi level and the Dirac point is about 300 meV. This indicates we are probing the electrons in our $BiSbTeSe_2$ devices far away from the zeroth LL. Therefore, the Zeeman effect in our $BiSbTeSe_2$ devices should be very small.

In addition, the Zeeman energy, $E_z = g_s \mu_B B$, is magnetic field tilting angle dependent[4,5]. It would induce a large deviation to the magnetoresistance curves at different tilting angles with respect to the zero-tilting case if the Zeeman energy is large. However, as shown in Figure 1(d), the ΔG_{xx} curves in tilted magnetic field collapse into that in perpendicular field, even at relatively large tilting angle, such as 60° and 70°. Such an observation further demonstrates that the Zeeman effect in our $BiSbTeSe_2$ devices can be neglected.

As a result, we believe that the Zeeman effect on the split of topological surface states in our $BiSbTeSe_2$ devices can be neglected to explain our experimental findings.

2. Temperature dependence of AMC magnitude

The angular dependence of AMC magnitude, defined as $\Delta G_{xx} = G_{xx}(\theta) - G_{xx}(0^o)$, is shown in Figure S1(a). The maximum AMC magnitude obtained in the parallel configuration (θ = 90°) decreases monotonically as temperature increases from 2 K to 300 K (Figure S1(b)).

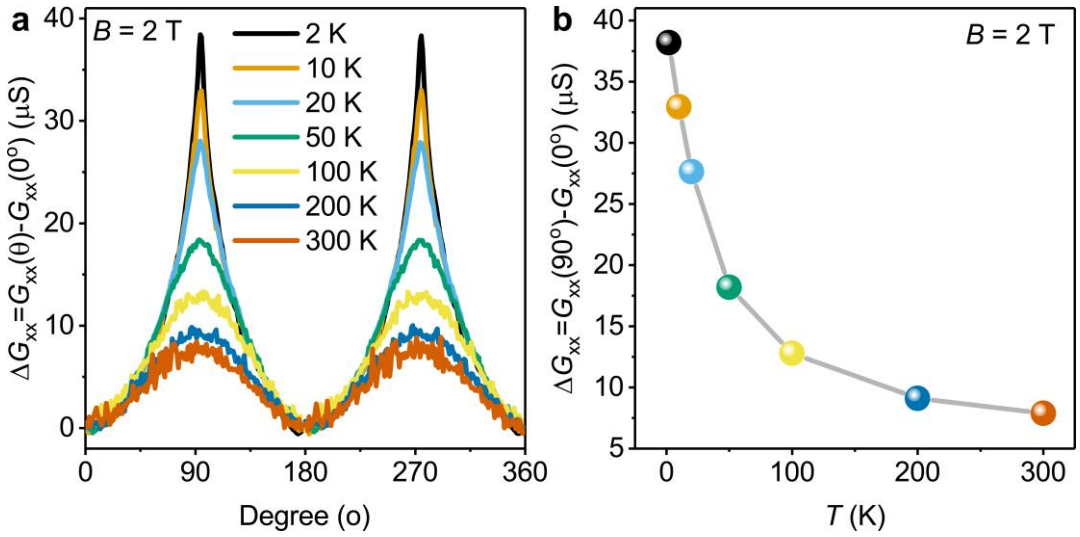

Figure S1. (a) The angular dependence of the AMC magnitude measured at B = 2 T and the various temperature indicated. (b) The temperature dependence of the AMC magnitude with θ = 90°.

3. ARPES measurements of the $BiSbTeSe_2$ single crystals

We have performed the angle-resolved photoemission spectroscopy (ARPES) measurements to investigate the electronic structure of our $BiSbTeSe_2$ single crystals after 10 hours aging. The ARPES was measured at 10 K. As shown in Figure S2 below, the typical bulk conduction band (BCB), surface state band (SSB) and bulk valence band (BVB) are observed clearly.

The Fermi level lies above and close to the bottom of the BCB, indicating the unintentionally *n*-doping of our $BiSbTeSe_2$ single crystals. This is consistent with our magnetotransport results presented in the main text, where both surface states and bulk states contribute to the AMC and the surface states contribution ratio increases after applying negative gate bias.

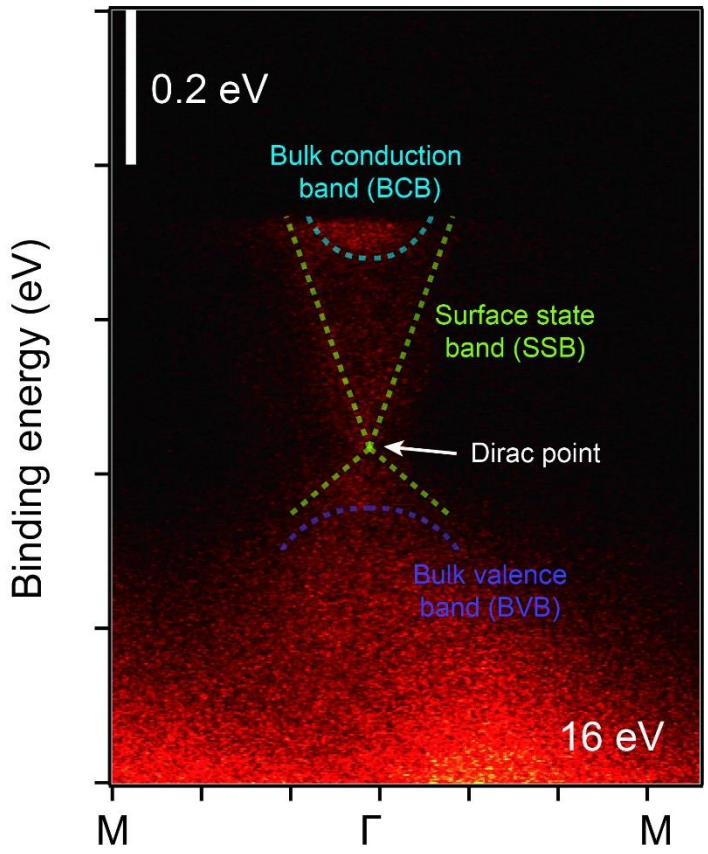

Figure S2. The ARPES measurements of $BiSbTeSe_2$ single crystals measured with an incident photon energy of 16 eV near the Γ-point along the M-Γ-M. The dashed lines are guides to the eyes.

4. Estimation of the standard error of the surface states contribution ratio

As shown in the main text, the surface states contribution ratio is given by

$$y = \frac{\Delta G_{xx}(0)}{G_{xx}(0)} \times 100\% = \frac{\alpha \frac{e^2}{2\pi^2\hbar}\left[\psi\left(\frac{1}{2}+\frac{\hbar}{4eBl_\phi^2}\right)-\ln\left(\frac{\hbar}{4eBl_\phi^2}\right)\right]}{G_\perp + \alpha \frac{e^2}{2\pi^2\hbar}\left[\psi\left(\frac{1}{2}+\frac{\hbar}{4eBl_\phi^2}\right)-\ln\left(\frac{\hbar}{4eBl_\phi^2}\right)\right]} \times 100\%$$

in which the α, $G_\perp$ and l_ϕ are the fitting parameters with the standard deviation listed in the following Tables S1-S3.

The standard deviation of the surface states contribution ratio *s* is then defined as

$$s^2 = \sqrt{\left(\frac{\partial y}{\partial \alpha}\right)^2 s_\alpha^2 + \left(\frac{\partial y}{\partial G_\perp}\right)^2 s_{G_\perp}^2 + \left(\frac{\partial y}{\partial l_\phi}\right)^2 s_{l_\phi}^2}$$

where s_α, $s_{G_\perp}$, and s_{l_ϕ} are the standard deviation of the fitted α, $G_\perp$ and l_ϕ. The calculated *s* is listed in following Tables.

Table S1 Fitting parameters for AMC at different *B*-fields (Figure 2(d)).

Parameters	2 T	4 T	6 T	8 T
α	-0.59±0.019	-0.58±0.017	-0.61±0.018	-0.63±0.027
$G_\perp$ (mS)	1.012±0.004	0.099±0.006	0.098±0.004	0.096±0.006
l_ϕ (nm)	163.073±6.822	136.223±5.926	129.466±5.954	127.76±9.143
ratio (%)	2.811±0.111	3.102±0.116	3.479±0.132	3.789±0.218

Table S2 Fitting parameters for AMC at different temperature measured at *B* = 2 T (Figure 3(c)).

Parameters	2 K	10 K	20 K
α	-0.590±0.019	-0.579±0.023	-0.620±0.028
$G_\perp$ (mS)	1.012±0.004	1.048±0.007	1.087±0.004
l_ϕ (nm)	163.073±6.822	118.144±5.153	76.2673±2.771
ratio (%)	2.811±0.111	2.246±0.110	1.641±0.094

Table S3 Fitting parameters for AMC at 3 T, 2 K and -2 V (Figure 5(b) and 5(c)).

Parameters	-2 V, 3 T
α	-0.470±0.040
$G_\perp$ (mS)	0.307±0.009
l_ϕ (nm)	237.830±3.198
ratio (%)	8.530±0.098

References

(1) Fu, Y.-S.; Hanaguri, T.; Igarashi, K.; Kawamura, M.; Bahramy, M. S.; Sasagawa, T. Observation of Zeeman effect in topological surface state with distinct material

dependence. *Nat. Commun.* **2016,** *7*, 10829.

(2) Xu, Y.; Miotkowski, I.; Liu, C.; Tian, J.; Nam, H.; Alidoust, N.; Hu, J.; Shih, C.-K.; Hasan, M. Z.; Chen Y. P. *Nat. Phys.* Observation of topological surface state quantum Hall effect in an intrinsic three-dimensional topological insulator. **2014,** *10*, 956–963.

(3) Zhang S., Pi L., Wang R., Yu G., Pan X.-C., Wei Z., Zhang J., Xi C., Bai Z., Fei F., Wang M., Liao J., Li Y., Wang X., Song F., Zhang Y., Wang B., Xing D., Wang G., Anomalous quantization trajectory and parity anomaly in Co cluster decorated $BiSbTeSe_2$ nanodevices, *Nat. Commun.* **2017,** *8*, 977.

(4) Dey, R.; Pramanik, T.; Roy, A.; Rai, A.; Guchhait, S.; Sonde, S.; Movva, H. C. P.; Colombo, L.; Register, L.F.; Banerjee S. K. Strong spin-orbit coupling and Zeeman spin splitting in angle dependent magnetoresistance of Bi_2Te_3 *Appl. Phys. Lett.* **2014,** *104*, 223111.

(5) Wang, L.-X.; Yan,Y.; Zhang, L.; Liao, Z.-M.; Wu, H.-C.; Yu, D.-P.; Zeeman effect on surface electron transport in topological insulator Bi_2Se_3 nanoribbons. *Nanoscale* **2015,** *7*, 16687.